

Supporting Information

The evolutions of Pt with different initial sizes during propane oxidation over Pt-CeO₂ catalysts

Jinshi Dong^{a*}, Shijun Huang^a, Shengtong Li^a, Panpan Chang^a, and Jiaqiang Yang^{b*}

^a Laboratory of New Energy and Environmental Catalysis, School of Biological and Chemical Engineering, Guangxi University of Science and Technology, Liuzhou 545006, Guangxi, China

^b Zhongyuan critical metals laboratory, Zhengzhou University, Zhengzhou 450001, Henan, China

* Corresponding author. E-mail addresses: jinshidong@gxust.edu.cn (J. Dong), jqyang@zzu.edu.cn (J. Yang).

Experimental section

1. Catalysts preparation

CeO₂ was prepared by calcining the Ce(NO₃)₃·6H₂O (99.5%, Macklin) in flowing air at 350 °C for 2 h and then at 500 °C for 3 h. 0.1wt% Pt (precursor: H₂PtCl₆·6H₂O, from Shanghai Aladdin Biochemical Technology Co., LTD) was supported on CeO₂ powder by incipient wetness impregnation method. After the sample was completely dried under infrared lamp, it was calcined in muffle furnace at 400 °C for 4 h. The obtained sample was denoted as 0.1Pt-CeO₂.

2. Characterization methods

Transmission electron microscopy (TEM) images were obtained using an aberration corrected JEM-ARM 200F (JEOL) field emission electron microscope. The catalyst powder was firstly dispersed in ethanol by ultrasonic treatment and then dropped on Cu grids.

CO-DRIFTS was conducted on a Nicolet iS50 FTIR spectrometer which is equipped with a Pike high temperature reaction chamber. In each ex-situ test, 20 mg catalyst was put into the sample storehouse and reduced at 150 °C in 10% CO/Ar at a flow rate of 100 mL/min for 10 min or at 350 °C in 5% H₂/Ar at a flow rate of 100 mL/min for 15 min. After the sample cooling to room temperature, Ar flow purged for 10 min and a spectrum was collected as background. Subsequently, 10% CO/Ar flow (50 ml/min) was supplied for 10 min and switched to Ar flow (100 ml/min) for 60s, after which the CO adsorption spectrum was collected. In each in situ reaction test, the pretreatment steps were the same as the above procedures. After cooling to room temperature, the reaction atmosphere fed and the sample was heated to target temperature for 60s. To avoid Pt sintering in Ar at high temperatures, the reaction atmosphere would be kept during the cooling process until the temperature decreased to 150 °C and then Ar was switched. The reaction atmosphere consisted of 0.1% C₃H₈ and 5% O₂ balanced with Ar at a total flow rate of 40 mL/min. After cooling to room temperature, the background spectrum was collected prior to each CO-DRIFTS spectrum being collected.

XPS tests were performed on a Thermo fisher Scientific K-Alpha spectrometer with Al K α (1486.6 eV) X-ray excitation source operated at 12 kV. The catalysts were rapidly transferred to vacuum tubes in glove box filled with Ar after being kept in the designed conditions. To avoid Pt states changing in ambient atmosphere, the samples were all put on the holder in glove box before XPS tests.

For O₂-TPD test, about 0.05g reduced catalyst was pretreated by 10%O₂/Ar at 300 °C for 1h. Then, the sample was cooling down to room temperature under Ar and kept for 1 h to clean

the physisorbed O₂. After that, the sample was heated from 30 to 450 °C at a ramping rate of 10 °C min⁻¹ to measure the desorbed O₂ (m/z=32) by using a mass spectrometer detector. For C₃H₈-TPD test, about 0.05g reduced catalyst was pretreated by 5% C₃H₈/Ar at ambient temperature for 1h. Then, the system was purged in a flow of Ar for 1 h. After that, the sample was heated to 500 °C at a ramping rate of 10 °C min⁻¹ to measure the desorbed C₃H₈ (m/z=29, the strongest ion signal) by a mass spectrometer detector .

3. Catalytic activity and kinetic tests

In a conventional C₃H₈ oxidation reaction test, 50 mg catalyst powder was firstly mixed with ~ 0.7g quartz sand and then placed in a U-type quartz tube reactor. The C₃H₈ oxidation light-off tests were performed with a ramping rate of 10 °C/min and heated to 450 °C. The reaction atmosphere consisted of 0.1% C₃H₈ and 5% O₂ balanced with Ar at a total flow rate of 100 mL/min. A HPR-20 R&D on-line mass spectrometer was used to monitor the C₃H₈, O₂ and CO₂ concentrations. Before tests, the catalysts were reduced at 150 °C in 10% CO/Ar at a flow rate of 100 mL/min for 10 min or at 350 °C in 5% H₂/Ar at a flow rate of 100 mL/min for 15 min. The obtained samples were denoted as 0.1Pt-CeO₂-150CO and 0.1Pt-CeO₂-350H₂. The kinetic measurements of C₃H₈ oxidation reaction were conducted with C₃H₈ conversion below ~ 20% to eliminate the thermal and diffusion effects.

4. Computational details

DFT calculations¹ were performed by Vienna Ab initio Simulation Package (VASP)²⁻⁵. The exchange and correlation energy was treated by generalized gradient approximation (GGA) with the Perdew-Burke-Ernzerhof (PBE)⁶ form generated using the projector augmented wave (PAW) method⁷. The DFT+U method was applied and the U value was set as 5.0 eV for the Ce 4f states^{8,9}. The energy cutoff was set as 400 eV, and the convergence criterion of geometry optimization was the maximum force on each atom less than 0.05 eV/Å. The 2 × 4 c(2 × 2) CeO₂ (111) surface with six atomic layers were cleaved from cubic CeO₂ unit cell. The vacuum layer between slabs was 15 Å and a 2 × 2 × 1 k-point mesh was used. The adsorbates and the top three layers were relaxed while the bottom three layers were fixed during the structural optimization. DFT-D3 method was used to correct the dispersion force.

To elucidate the origins of different evolution behaviors of initial Pt single atoms and Pt nanoparticles during C₃H₈ oxidation, the adsorption energies of reactant molecules on Pt surface were calculated. The adsorption energy of gas molecule is defined as:

$$E_{m/Pt_n-CeO_2}^{ads} = E_{m/Pt_n-CeO_2} - E_{Pt_n-CeO_2} - E_m \#(1)$$

where *m* and *n* are the gas molecule (C₃H₈ or O₂) and the number of Pt atom (*n* = 1, 2, 13),

respectively. Where E_{m/Pt_n-CeO_2} , $E_{Pt_n-CeO_2}$ and E_m are the ground state energies of the gas molecule adsorbing on Pt_n-CeO_2 , Pt_n-CeO_2 and gas molecule, respectively. The adsorption energy at certain temperature and pressure is defined as:

$$E_{m/Pt_n-CeO_2}^{ads}(T, P) = E_{m/Pt_n-CeO_2}^{ads} + \Delta G_{m/Pt_n-CeO_2}^{ads}(T, P) - \mu_m(T, P) \quad (2)$$

where $\Delta G_{m/Pt_n-CeO_2}^{ads}(T, P)$ is the Gibbs free energy of the gas molecule adsorbing on Pt_n-CeO_2 at certain temperature and pressure, $\mu_m(T, P)$ is the chemical potential of the gas molecule at certain temperature and pressure. Here, the C_3H_8 oxidation reaction was carried out under atmospheric pressure, $P = 1$ atm. The chemical potential of gas molecule at ground state is defined as zero.

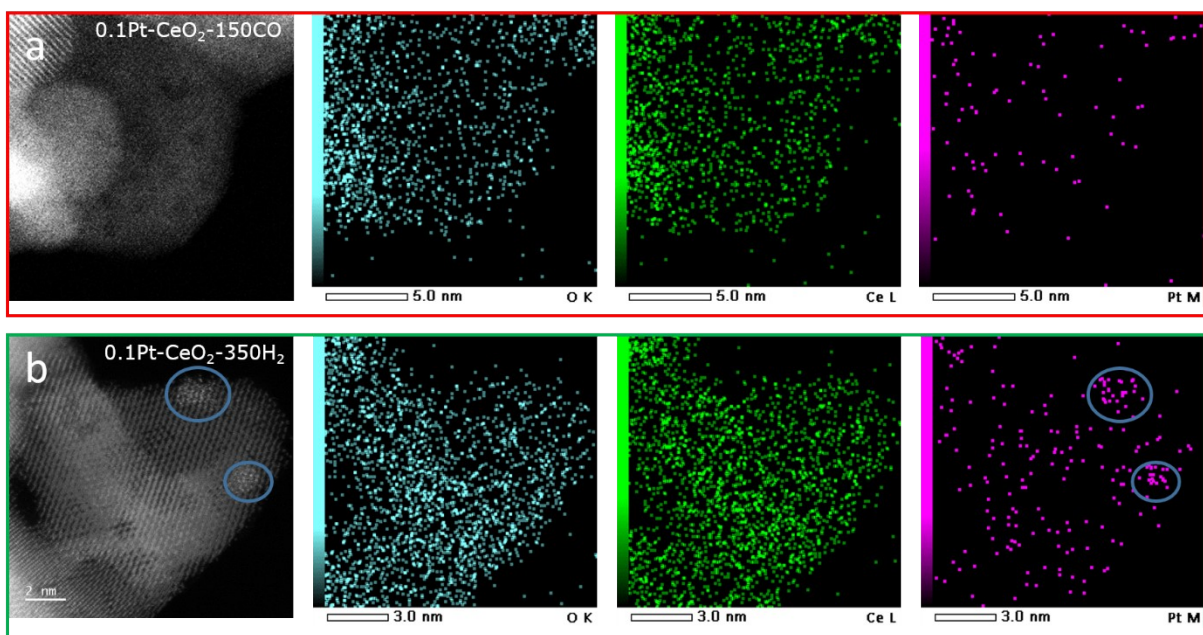


Fig. S1 HAADF-TEM and element mapping images of (a) CO-reduced and (b) H₂-reduced 0.1Pt-CeO₂ catalyst.

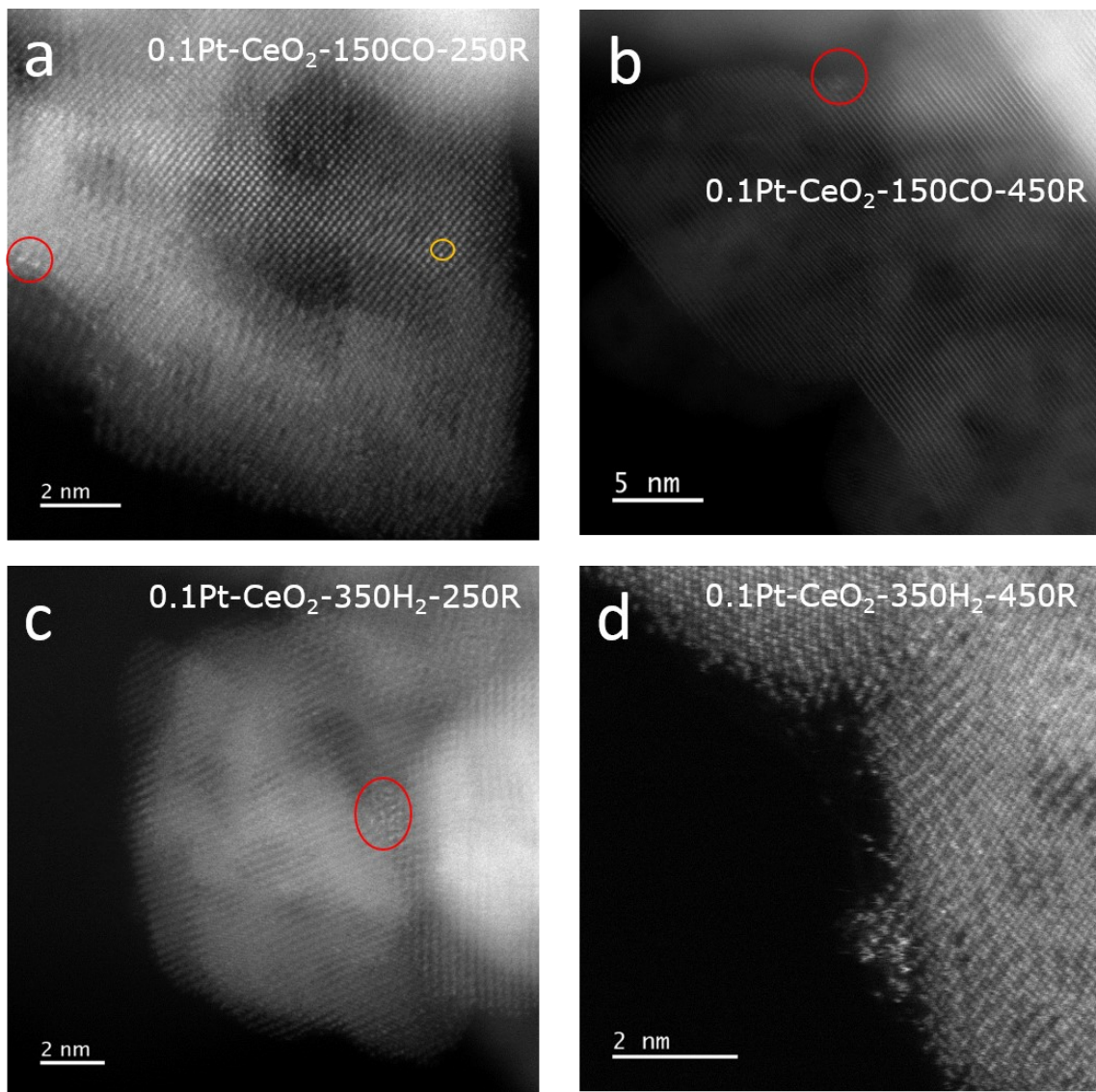


Fig.S2 TEM images of (a), (b) CO-reduced and (c), (d) H₂-reduced 0.1Pt-CeO₂ catalyst after C₃H₈ oxidation reaction at different temperatures.

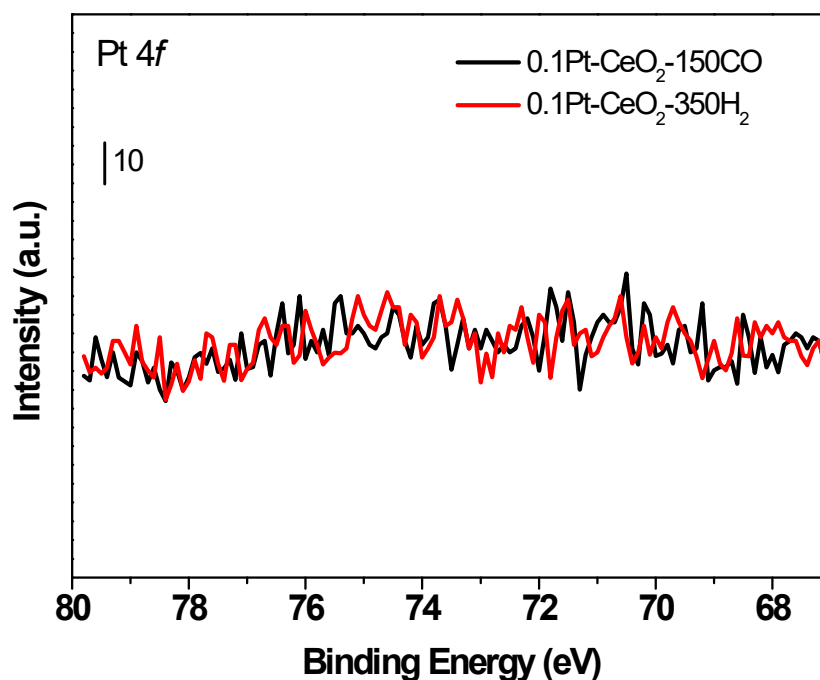


Fig.S3 NAP-XPS spectra of CO-reduced and H₂-reduced 0.1Pt-CeO₂ catalysts tested on a SPECS NAP-XPS equipment under an UHV environment of 5E-9 mbar at Nano-X platform from Suzhou Institute of Nano-Tech and Nano-Bionics, Chinese Academy of Sciences (SINANO).

It can be found no obvious Pt signals were collected in this NAP-XPS equipment even in the UHV condition as high as $\sim 5E-9$ mbar, let alone in C₃H₈ oxidation atmosphere under the vacuum of several mbar. Because of the light gun and signal collection system of NAP-XPS equipment are redesigned which are different from those of conventional XPS equipment to get clear signals in a certain atmosphere under the working condition of several mbar. As a result, conventional XPS equipment can obtain a much stronger intensity in signal than that of NAP-XPS equipment under the same UHV condition.

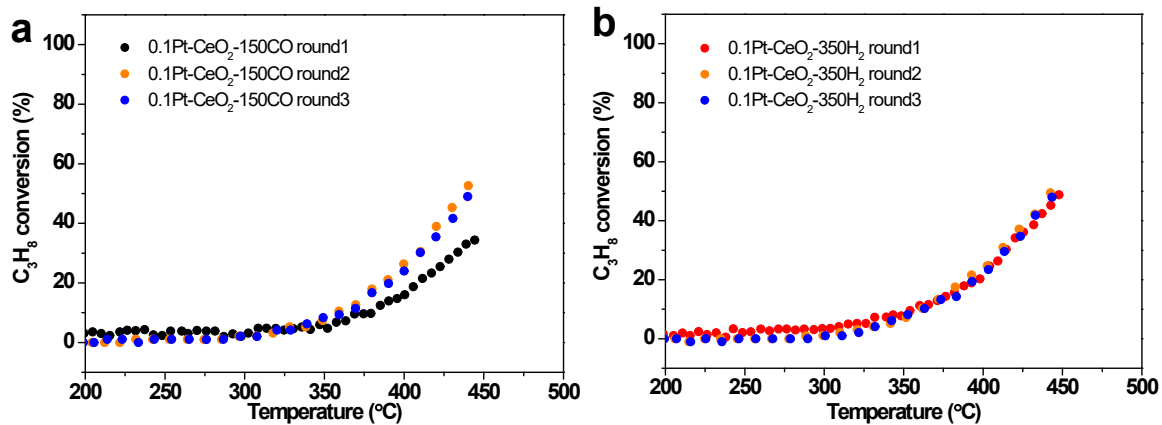


Fig. S4 C₃H₈ oxidation light-off curves of (a) 0.1Pt-CeO₂-150CO and (b) 0.1Pt-CeO₂-350H₂ catalysts for three rounds. Reaction conditions: 0.1% C₃H₈ and 5% O₂ balanced with Ar at a total flow rate of 100 mL/min. The catalyst dosage for each sample was 50 mg.

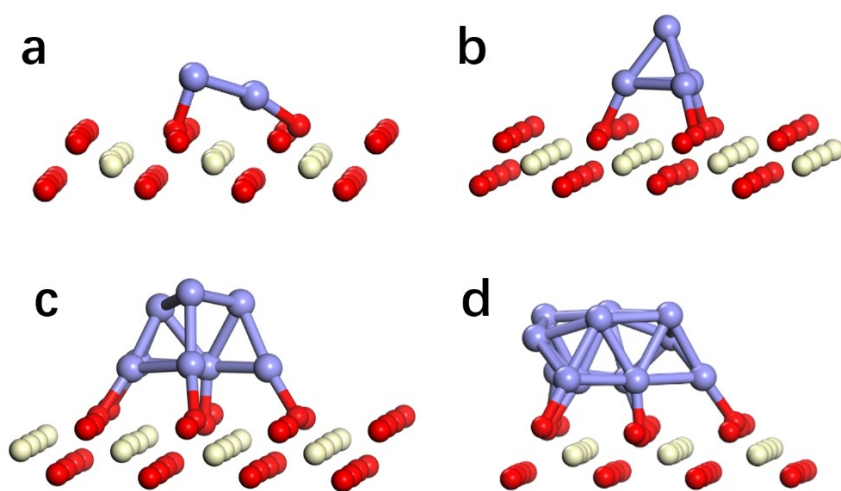


Fig. S5 The relaxed structures (a) Pt₂ dimer (b) Pt₄ cluster (c) Pt₈ and (d) Pt₁₃ ensemble on CeO₂ (111) facet.

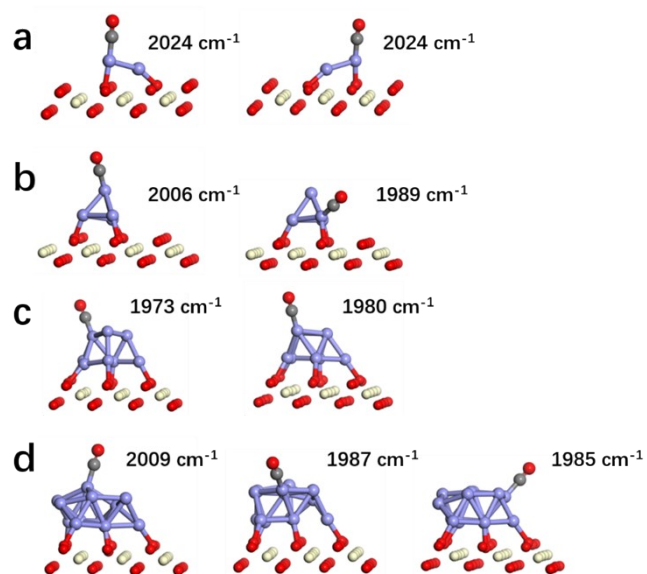


Fig. S6 Relaxed structures of CO linear adsorbed on (a) Pt2 dimer (b) Pt4 cluster (c) Pt8 and (d) Pt13 ensemble at different sites and the corresponding CO stretching frequencies by DFT calculations.

Table S1 Comparison of the catalytic performance in this work with those recent work in the literature for propane oxidation.

Catalyst	React. temp. (°C)	Reaction rate ($\mu\text{mol g}_{\text{Pt}}^{-1} \text{s}^{-1}$)	Reference
1%Zr-Co ₃ O ₄	185	9.0($\text{g}_{\text{Zr}}^{-1}$)	Appl. Catal. B: Environ. 298 (2021) 120606
1%Pd-CeO ₂ -O	300	80.8($\text{g}_{\text{Pd}}^{-1}$)	ACS Catal. 6(2016) 2265–2279
0.2Pt/BN	220	92.3	ACS Catal. 9(2019)1472-1481
1Pt-7W/BN	220	367.1	Appl. Catal. B: Environ. 272(2020) 118858
0.25Pt-CeO ₂ (NL)-750	300	160.9	J. Catal. 407(2022) 174-185
0.1Pt-CeO ₂ -350H ₂	350	132.4	This work

References:

1. Kohn, W.; Becke, A. D.; Parr, R. G., Density Functional Theory of Electronic Structure. *The Journal of Physical Chemistry* **1996**, *100*, (31), 12974-12980.
2. Kresse, G.; Hafner, J., Ab initio molecular dynamics for liquid metals. *Physical Review B* **1993**, *47*, (1), 558-561.
3. Kresse, G.; Hafner, J., Ab initio molecular-dynamics simulation of the liquid-metal–amorphous-semiconductor transition in germanium. *Physical Review B* **1994**, *49*, (20), 14251-14269.
4. A, G. K.; b, J. F., Efficiency of ab-initio total energy calculations for metals and semiconductors using a plane-wave basis set *Computational Materials Science* **1996**, *6*, (1), 15-50.
5. Kresse, G.; Furthmüller, J., Efficient iterative schemes for ab initio total-energy calculations using a plane-wave basis set. *Physical Review B* **1996**, *54*, 11169–11186
6. Perdew, J. P.; Burke, K.; Ernzerhof, M., Generalized Gradient Approximation Made Simple. *Physical Review Letters* **1996**, *77*, (18), 3865-3868.
7. Blöchl, P. E., Projector augmented-wave method. *Physical Review B* **1994**, *50*, (24), 17953-17979.
8. Zhou, Q.; Zhou, C.; Zhou, Y.; Hong, W.; Zou, S.; Gong, X.-Q.; Liu, J.; Xiao, L.; Fan, J., More than oxygen vacancies: a collective crystal-plane effect of CeO₂ in gas-phase selective oxidation of benzyl alcohol. *Catalysis Science & Technology* **2019**, *9*, (11), 2960-2967.
9. Kim, H. Y.; Lee, H. M.; Henkelman, G., CO oxidation mechanism on CeO₂-supported Au nanoparticles. *J Am Chem Soc* **2012**, *134*, (3), 1560-1570.